Modelling, Simulation and Characterization ZnO Piezoelectric Thin Films for FBAR

Roger Ondo Ndong[1,2*], Honoré Gnanga[1], Jean Aubin Ondo[1] and Alain Foucaran[2]

1. Laboratoire pluridisciplinaire des Sciences, LAPLUS, Ecole Normale Supérieure, BP 17009

Libreville Gabon

2. Institut Electronique du Sud, IES-Unité mixte de Recherche du CNRS n° 5214, Université Montpellier II, Place E. Bataillon, 34095 Montpellier cedex 05- France.

Abstract

Characteristics of Zinc oxide (ZnO) piezoelectric thin films have been investigated for thin film bulk acoustic resonators (FBAR) with relationship to bottom electrodes. Several critical parameters of the RF magnetron sputtering process deposition pressure, RF power, substrate temperature, O_2 concentration and the target to substrate distance were determined to clarify their effects on the material characteristics of the ZnO. Highly c-axis oriented thin films as thick as 5.7 µm were grown and analyzed. Compressive stresses were observed. The FBAR devices with the ZnO films exhibited a pronounced resonance peak centred at 790 MHz with a k^2 coupling coefficient of 7 %. It found therefore that the impedance matching of the FBAR could be easily achieved simply by controlling the resonance the resonator

1. Introduction

Bulk acoustic wave (BAW) resonators using piezoelectric thin film are valuable devices for high frequency telecommunications [1]. Many studies of BAW devices have been carried out in recent years [2-6]. ZnO thin film is a practical piezoelectric material for applications to BAW and surface acoustic wave (SAW) devices for its large electro-mechanical coupling coefficient. It is very important to improve the resonant characteristics of BAW resonator to be adopted for telecommunication devices that have severe specifications for electrical characteristics. We have investigated ZnO piezoelectric thin films and their microstructure for SAW and BAW devices [7-8]. The most critical factor determining the resonance characteristics of FBAR devices is piezoelectric properties of the ZnO films, which is directly related to degree of the preferred orientation of the Zno crystal structure [9-10]. Considerable effort has been made to fabricate high quality ZnO films with a strongly preferred orientation. However, each approach has shown its own limitations such as the complexity of the fabrication methods and the high cost of process equipment. In FBAR devices, the ZnO film should exert a minimum stress on the underlying layer and also have a high piezoelectric constant.

This paper presents the modeling; simulation and the analysis of ZnO based FBAR's that are centred at frequencies ranging from 300 to 2 GHz. The texture of zno thin film was analyzed by X-ray diffraction and the electromechanical coupling coefficient k^2 was measured with Network analyzer. On the other hand the electrical properties of the resonators were measured and are discussed as function of materials parameters and processing conditions.

2. Zinc oxide thin films

Zinc oxide films were deposited by r.f magnetron sputtering using a zinc target (99,99%) with diameter of 51 mm and 6 mm thick. Substrate is p-type silicon with (100) orientation. The substrates were thoroughly cleaned with organic. Magnetron sputtering was carried out in oxygen and argon mixed gas atmosphere by supplying r.f power at a frequency of 13.56 MHz. The RF power was about 50 W. The flow rates of both the argon and oxygen were controlled by using flow meter (ASM, AF 2600). The sputtering pressure was maintained at $3.35.10^{-3}$ torr controlling by a Pirani gauge. Before deposition, the pressure of the sputtering system was under 4.10-6 torr for more than 12 h and were controlled by using an ion gauge controller (IGC – 16 F). Thin films were deposited on silicon, substrate under conditions listed in Table 1 [11]. These deposition conditions were fixed in order to obtain the well-orientation zinc oxide films. The presputtering occurred for 30 min to clean the target

surface. Deposition rates covered the range from 0.35 to 0.53μm/h. All films were annealed in helium ambient at 650°C for 15mn. In this study Pt was chosen as a bottom electrode material for the FBAR fabrication. In order to investigate the crystallographic properties of the ZnO films, we carried out an X-ray diffraction (XRD) analysis using CuKα (λ = 0,154054 nm) radiation. The diffractogram of a 5.7 μm ZnO thin film deposited on a platinized substrate. No other peak than the (002) one could be detected, indicating a very good c-axis texture. The dielectric properties of Zno films were measured with an impedance analyzer. Typical values for the relative permittivity and the dielectric losses were 8.5 and 0.002 respectively.

Table 1: ZnO sputtering conditions

Sputtering pressure	3.35×10^{-3} Torr
Mixture gas	Ar + O_2 = 80 – 20 %
Power RF	50 W
Sputtering time	6 h
Substrate temperature	100 °C
Target-substrate distance	7 cm

3. Theoretical consideration

Throughout piezoelectric material, there is interdependence between mechanical and electrical quantities. This implies a coupling between elastic waves and electromagnetic waves. From the two solutions of the wave equation, it is possible to write linear relationships between the mechanical (strength and speed) and electrical parameters (voltage U and current I injected).The presentation of these relations in matrix form then allows deducing the equivalent electromechanical schemes.

3.1. Impedance matrix

Consider a piezoelectric slice thickness and A section subjected to an electrical voltage U and the forces F1 and F2 (Figure 1). The forces F1 and F2 exerted on each of the faces and the velocities v1 and v2 entering a play similar to that of the voltage and the current roll.

The forces F1 and F2 are written:

$$\begin{cases} F_1 = -AT(x_1) \\ F_2 = AT(x_2) \end{cases}$$

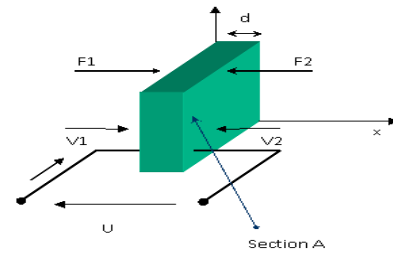A represents the cross section and the constraint T

Fig. 1: Slice of piezoelectric material section A

The constraint T for a piezoelectric material is written:

$$T = c\frac{\partial u}{\partial x} - hD \qquad (1)$$

With, the displacement u, c induction constant rigidity, D electrical induction and h ratio of the piezoelectric coefficient of the dielectric constant: $h = e/\varepsilon_s$

Deriving the expression (1) with respect to time, by considering the equation of conservation of charge

$$\partial D/\partial t = J(t) = I(t)/A$$

and indicating the speed of the particles $v = \partial u/\partial t$, it is found that: $\dfrac{\partial T}{\partial t} = c\dfrac{\partial v}{\partial x} h\dfrac{\partial D}{\partial t} = c\dfrac{\partial v}{\partial x} - \dfrac{h}{A}I(t)$ (2)

Moreover the propagation equation is of the form:

$$\rho\frac{\partial^2 v}{\partial t^2} = c\frac{\partial^2 v}{\partial x^2}$$

The general solution of this equation is the harmonic sum of two waves propagating in opposite directions (the speed $V = \sqrt{c/\rho}$): $v = ae^{-ikx} + be^{ikx} = v_a + v_b$ (3)

with $k = w/V$

The constraint expression is derived from the expression (2) by plotting the expression (3) speed:

$$T = -Z(a.e^{-ikx} - b.e^{ikx}) + i\frac{h}{Aw}I$$

From the expression of the stress and remembering that the mechanical impedance can be written Z = ZA (where Z is the characteristic impedance and A section of the piezoelectric segment bounded by the planes x = x_1 and x = x_2), we deduce that the forces F_1 and F_2 are then written in the form:

$$\begin{cases} F_1 = -AT(x_1) = Z\left(ae^{-ikx_1} - be^{ikx_2}\right) - i\dfrac{h}{w}I \\ F_2 = AT(x_2) = Z\left(ae^{-ikx_2} - be^{ikx_2}\right) - i\dfrac{h}{w}I \end{cases}$$

The relation (3) can write that

$$\begin{cases} v_1 = v(x_1) = ae^{-ikx_1} - be^{ikx_2} \\ v_2 = -v(x_2) = -ae^{-ikx_2} - be^{ikx_2} \end{cases}$$

Where one draws the expressions of coefficients:

$$a = \frac{v_1 e^{-ikx_2} + v_2 e^{ikx_1}}{2i\sin(kd)} , \quad b = -\frac{v_2 e^{-ikx_1} + v_1 e^{ikx_2}}{2i\sin(kd)}$$

By feeding back these coefficients in (Syst.1), we find expressions connecting v_1, v_2 and I to F_1 and F_2:

$$F_1 = Z\left[\frac{v_1}{i\tan kd} + \frac{v_2}{i\sin kd}\right] - i\frac{h}{w}I \quad (4)$$

$$F_2 = Z\left[\frac{v_1}{i\sin kd} + \frac{v_2}{i\tan kd}\right] - i\frac{h}{w}I \quad (5)$$

Both acoustic access being characterized, it remains to find the expression that defines the electrical access. U voltage appearing between the two sides of the section A is expressed

$$U = \int_{x_1}^{x_2} E.dx$$

The electric field is derived from one of the two states of the piezoelectric equations, namely

$$D = \varepsilon_s E + e\frac{\partial u}{\partial x} \Rightarrow E = -h\frac{\partial u}{\partial x} + \frac{D}{\varepsilon_s}$$

Introducing the speed

$$v_1 = iwu(x_1) \text{ and } v_2 = iwu(x_2)$$

the voltage U becomes:

$$U = \frac{h}{w}(v_1 + v_2) + \frac{Id}{iwC_0} \quad (6)$$

Writing in matrix form equations (4), (5) and (6), shows the electromagnetic impedance matrix

$$[Z].\begin{bmatrix} F_1 \\ F_2 \\ U \end{bmatrix} = -i \begin{bmatrix} \dfrac{Z}{\tan kd} & \dfrac{Z}{\sin kd} & \dfrac{h}{w} \\ \dfrac{Z}{\sin kd} & \dfrac{Z}{\tan kd} & \dfrac{h}{w} \\ \dfrac{h}{w} & \dfrac{h}{w} & \dfrac{1}{wC_0} \end{bmatrix} \times \begin{bmatrix} v_1 \\ v_2 \\ I \end{bmatrix} \quad (7)$$

3.2. Masson and Redwood model

When the material is piezoelectric, there is an additional force must be taken into account in terms of F_1 and F_2.

The equivalent circuit diagram of a portion of piezoelectric solid is obtained by juxtaposing the equivalent of non-piezoelectric contrasts with the electromechanical transformer scheme.
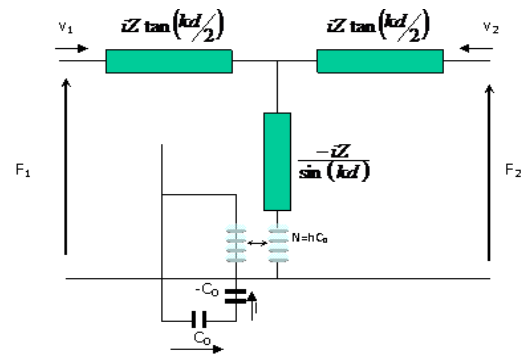

Fig. 2: Equivalent Mason model for piezoelectric

We consider for simulation, that the vibrations of the piezoelectric material will generate only longitudinal waves or only transverse waves. This will provide a model that is valid and consistent with reality.

The electrical input impedance of the computed from the matrix (7) is [12, 13] structure:

$$Z_e = \frac{1}{iC_0 w}\left(1 + \frac{K^2 Z}{\varphi} \times \frac{2Z(1-\cos\varphi) - i(Z_1+Z_2)\sin\varphi}{-(Z^2+Z_1 Z_2)\sin\varphi + iZ(Z_1 Z_2)\cos\varphi}\right) \quad (8)$$

Z_p, Z_1, Z_2 each represents the acoustic impedances of the piezoelectric material, settings on the front and rear of the piezoelectric material. k^2 represents the electromechanical coupling coefficient. Around the resonance this resonator can be represented by the following equivalent circuit:
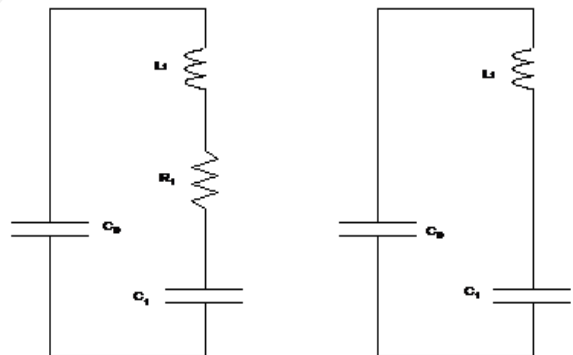

Fig.3: Electrical equivalent circuit of a piezoelectric resonator.

a) Model Mason, b) Piezoelectric free.

C_0 is the ability of the dielectric ZnO, L_1 represents the inertia of the circuit structure, friction losses R C_1 and the stiffness of the system. This circuit is an ideal model to represent the physical characteristics of a free resonator. Frequencies parallel and series resonance circuit can be written:

$$f_s = \frac{1}{2\pi\sqrt{L_1 C_1}} \text{ and } f_p = \frac{1}{2\pi\sqrt{L_1 \dfrac{C_1 C_0}{C_1 + C_0}}} \quad (9)$$

IEEE standard [13] shows that the coupling coefficient k^2 is given by

$$k^2 = \frac{\varphi}{\tan\varphi} \quad \text{with} \quad \varphi = \frac{\pi}{2}\frac{f_s}{f_p} \qquad (10)$$

This formula can be written in a more explicit approximate shape and then the error introduced by the approximation is less than 1% in the case where $k^2 < 0.2$, either:

$$k^2 = \frac{\pi^2}{4}\frac{f_s}{f_p}\left(1 - \frac{f_s}{f_p}\right) \qquad (11)$$

This means that we can calculate the coupling coefficient k^2 just under the maximum real part of the impedance and admittance. Indeed, one can simply raise the maximum values of resistance (impedance) and conductance (admittance) to the resonant frequency when the imaginary parts are zero.

Using equation (8), we plot the theoretical evolution of the real and imaginary parts of the electrical admittance of the open resonator of 5.7μm thick, depending on the frequency (Figure 4)
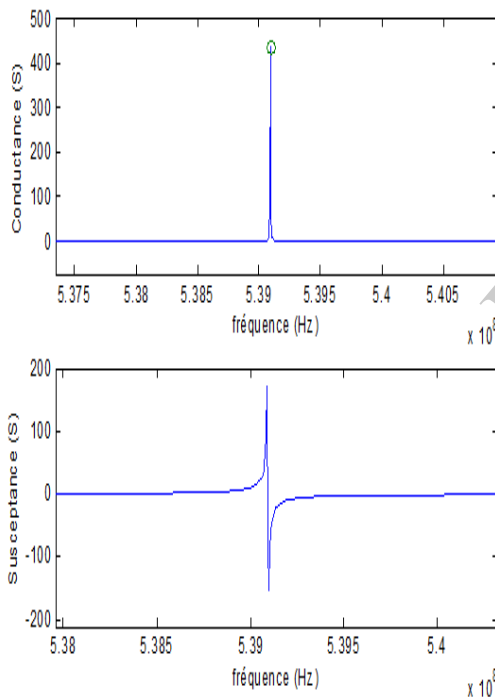

Fig.4: Frequency dependence of the admittance of free resonator

4. Results

The structure comprises a piezoelectric material having two electrodes (silver and titanium / platinum) on each side. The electric field of the signal applied between the electrodes to vibrate the piezoelectric puts solid (ZnO). The vibrations are propagated in a medium mechanically secured (silicon) of the faces of a piezoelectric solid.
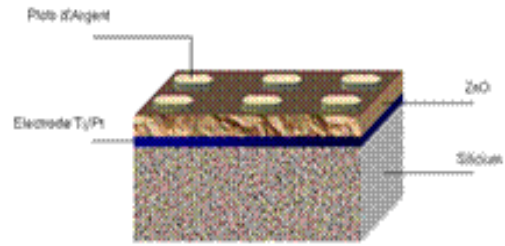

Fig.5: Studied structure

In the general case of a piezoelectric solid, note that the essential condition for validity based on those Masson, given the fact that they are one-dimensional models, there is generation of single mode propagation.

Gold in the zinc oxide, so as to enhance a longitudinal propagation mode, it is necessary that the axis of symmetry of order 6 is parallel to the electric field. Various experimental studies [11] have to control the orientation of the deposited layers, playing on various deposition parameters.

Based on the equivalent model of Masson we get the result in Figure 6 where the reflection coefficient is plotted against the frequency linear. We have also shown in the Smith chart of Figure 7
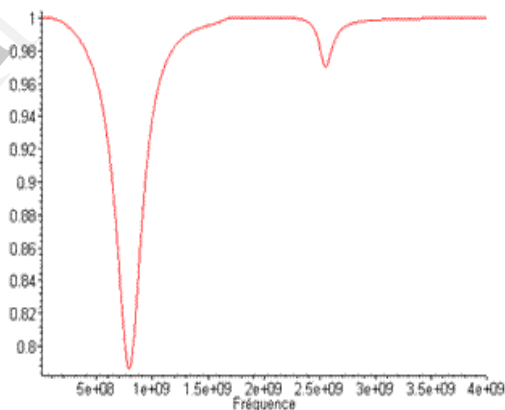

Fig. 6: Variation of reflection coefficient as function of the frequency
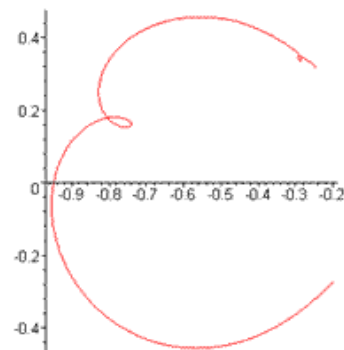

Fig.7: Polar representation of the real and imaginary parts of the reflection coefficient

By plotting the admittance as a function of frequency and comparing the same conditions the graphs

corresponding to the infinite and finite media spread, we see in the second case the appearance of ringing Figure 8. However, the major problem lies in the fact that uses a near-perfect model is therefore very far from reality.

This explains why on-oscillations seem to have infinite amplitude around the inflection point which corresponds to the natural resonance of ZnO.
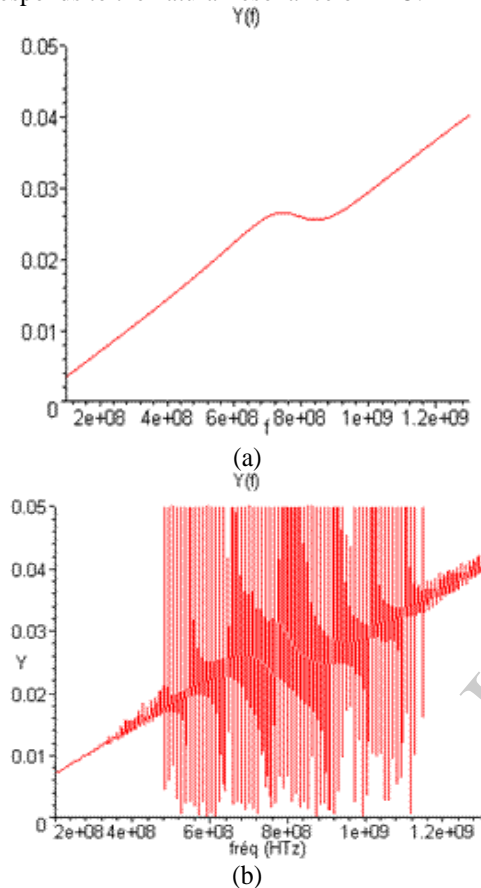

Fig.8: Admittance function frequency (a) infinite medium, (b) finite medium

We integrate the phenomena of dispersion and attenuation of the ultrasonic waves. These phenomena are mainly due either to absorption or diffraction of a medium. We used the imaginary propagation speeds to simulate phenomena. The velocity V, clean the material, an expression of the form replace $V(1+k*i)$, k corresponds somehow to the attenuation parameter (0 <k <0.1) Taking into account the viscoelastic phenomena is primarily a means of refine the modeling and thus get closer to a real case in Figure 9
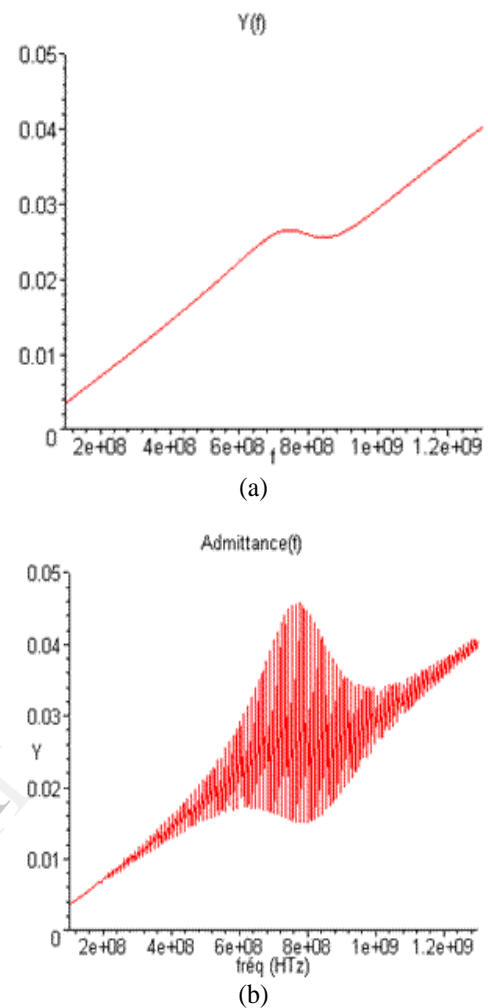

Fig.9: Admittance function frequency (a) infinite medium, (b) finite medium

We plotted the frequency dependence of the admittance of the resonator for a fundamental longitudinal mode. We observe that the evolution of the frequency dependence of the admittance differs markedly from the previous case. There is recombination of waves propagating in the two directions of the delay line, which leads to significant variations in the acoustic impedance returned to the surface of the piezoelectric element.

Also, by studying the variation of the reflection coefficient as a function of frequency in linear coordinates and polar coordinates, we obtain, respectively, the results of Figure 10 and Figure 11. For a thickness of 5.7μm ZnO and the silicon substrate 380μm, we observe the resonance at 790MHz. This confirms the good quality of zinc oxide produced for use or FBAR filters.
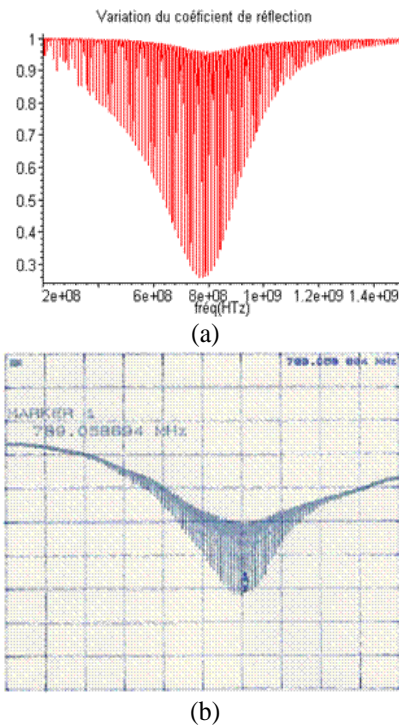
(a)

(b)

Fig.10: Reflection coefficient as a function of frequency. (a) simulation, (b) testing
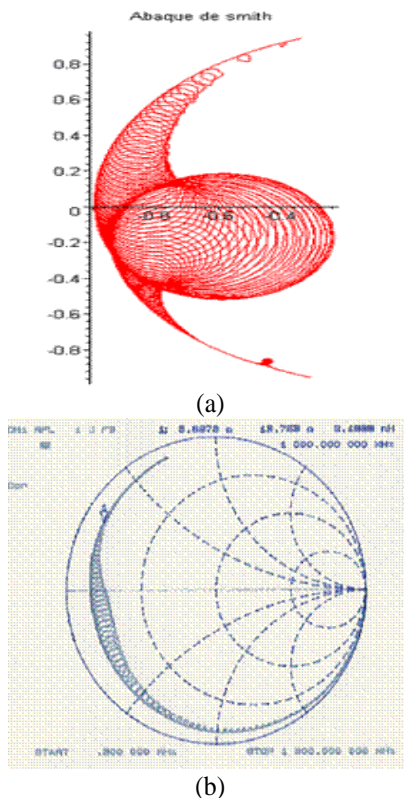

(a)

(b)

Fig.11: Reflection coefficient as a function of frequency in polar coordinate.
(a) Simulation, (b) testing

These impedance variations we observe are oscillations of frequency intervals Δf. They result in the occurrence of significant changes in the real and imaginary parts of the admittance measured in peak shape as shown in Figure 12.

These fluctuations occur with a periodicity Δf satisfying the expression that gives the resonant frequency of a vibrating cavity thickness mode. We found experimentally that the frequency of ringing for an 11MHz value. And this result is confirmed by simulation.

These changes affect the shape of the electrical admittance. But, the existence of losses the delay line and the transducer causing attenuation of amplitudes of peaks. These attenuations are due either to the diffraction of the mechanical wave in the substrate which forms an energy reservoir or with relaxation of the coefficient of stiffness of the atoms constituting the substrate.
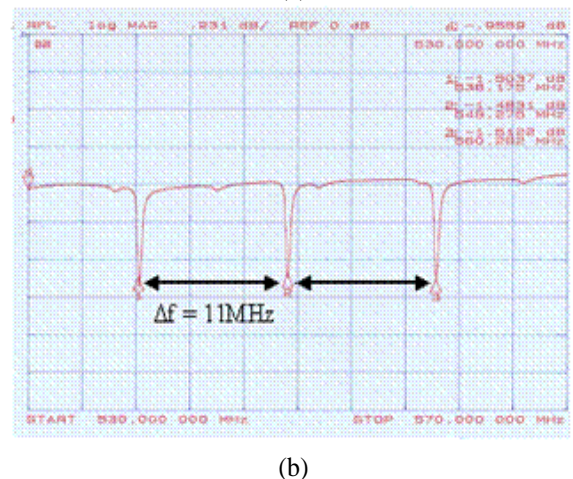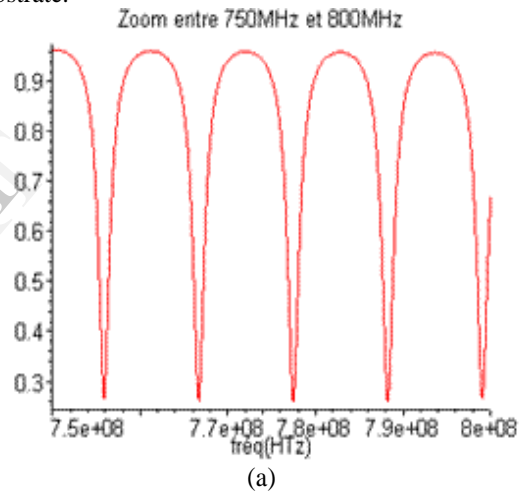

(a)

(b)

Fig.12: frequency of ringing. (a) Simulation, (b) testing

5. Conclusions

After presenting the basic equations governing piezoelectricity, we described the characteristics of a vibrating piezoelectric structure in compression mode. At first, we studied in detail the equivalent circuit diagram of a free resonator composed of a piezoelectric ZnO layer which both sides are metalized. We have thus determined the relationship between the electrical impedance at the frequency. From this relationship, we modelled our structure. The theoretical results were compared with experimental results and give a good agreement with respect to the resonance frequency and the effective coupling coefficient of the structure.

The FBAR devices with the ZnO films exhibited a pronounced resonance peak centred at 790 MHz with a k^2 coupling coefficient of 7 %. The above result demonstrates that the fabricated FBAR with excellent performance will be promising for high frequency applications.

6. References

[1] R. Ruby, P. Bradley, J. D. Larson III and Y. Oshmyansky, Electronics Letters, **35**, 794 (1999).

[2] T. R. Sliker and D. A. Roberts, J. Appl. Phys., **5**, 2350 (1967).

[3] K. M. Lakin and J. S. Wang, Appl. Phys. Letters, **38**, 125 (1980).

[4] Y. Miyasaka, S. Hoshino and S. Takahashi, Jpn. J. Appl. Phys. Suppl., **23**, 119 (1983).

[5] K. Nakamura, Y. Ohashi and H. Shimizu, Jpn. J. Appl. Phys., **25**, 371 (1986).

[6] J. Shiokawa, Y. Makishima, K. Hashimoto and M. Yamaguchi, Jpn. J. Appl. Phys., **32**, 2321 (1993).

[7] Y. Yoshino, T. Makino, Y. Katayama and T. Hata in *the 5th international Symposium of Sputtering and Plasma Processes* (Proc., Kanazawa, Japan, 1999), 233-234.

[8] Y. Yoshino in *Microelectromechanical Structures for Materials Research*, edited by S. Brown, J. Gilbert, H. Guckel, R. Howe, G. Johnson, P. Krulevitch and C. Muhlstein (Mater. Res. Soc. Proc. **518**, Pittsburgh, PA, 1998), 9-14.

[9] S. Fujishima, T. Kasanami, T. Nakamura, (1983). "Piezoelectric thin films and their applications for electronics" *Jpn. J. Appl. Phys*.22 p. 150.

[10] Pinkett SL, Hunt WD, Barber BP, Gammel PL, (2002). "Determination of ZnO temperature coefficients using thin film bulk acoustic wave resonators",*IEEE Trans Ultrason Ferroelectr Freq Control.*

Nov;49(11):1491-6.

[11] R. Ondo-Ndong, F. Pascal-Delannoy, A. Boyer, A. Giani, A. Foucaran, (2003). Structural properties of zinc oxide thin films prepared by r. f. magnetron sputtering", *Mat. Sci. Eng*. B97 P. 68.

[12] D. Royer, E. Dieulesaint, « Ondes élastiques dans les solides »,Tome 2, ed. Masson (1996).

[13] IEEE standard on piezoelectric IEEE / ANSI std. 176 (1987).